EurJIC
European Journal of Inorganic Chemistry

A Journal of
ChemPubSoc Europe

Accepted Article

Title: Long-range anti-ferromagnetic order on spin ladders SrFe2S2O and SrFe2Se2O, as probed by neutron diffraction and Mössbauer spectroscopy.

Authors: Hanjie Guo, Maria-Teresa Fernández-Díaz, Alexander Christoph Komarek, Sungjoon Huh, Peter Adler, and Martin Valldor

To be cited as: *Eur. J. Inorg. Chem.* 10.1002/ejic.201700684

Link to VoR: http://dx.doi.org/10.1002/ejic.201700684

WILEY-VCH

WILEY-VCH

FULL PAPER

Long-range anti-ferromagnetic order on spin ladders $SrFe_2S_2O$ and $SrFe_2Se_2O$, as probed by neutron diffraction and Mössbauer spectroscopy.

Hanjie Guo,[a] Maria-Teresa Fernández-Díaz,[b] Alexander Christoph Komarek,[a] Sungjoon Huh,[c] Peter Adler,[a] Martin Valldor*[a,d]

Abstract: Powder neutron diffraction data on spin ladder compounds $SrFe_2Ch_2O$ (*Ch* = S, Se) indicate that their magnetic ground states feature long range anti-ferromagnetic spin ordering with k = [0,0,0]. The super-exchange interaction is antiferromagnetic across each rung via oxygen but ferromagnetic along the ladders via *Ch*. At 10 K, the ordered spins point towards the center of the ladders but are faintly canted away from a collinear state. The sizes of the ordered moments are 3.3 and 3.5 μ_B Fe^{-1} for $SrFe_2S_2O$ and $SrFe_2Se_2O$, respectively. The polar, heteroleptic, tetrahedral $FeCh_3O$ coordination suggests an angle of 8° between the local structure polarity and the magnetic moment spin orientation. Mössbauer data confirm the magnetic ordering scenario and indicate that the local Fe–O bond rules the electric field gradient at the Fe-site.

Introduction

Low-dimensional iron lattices in solid-state chalcogenides attract more attention since the discovery of superconductivity in layered β-FeSe[1] and in the high-pressure state of the spin-ladder compound $BaFe_2S_3$.[2] In the chemically related compounds $AEFe_2Ch_2O$ (*AE* = Ba, Sr; *Ch* = S, Se),[3-6] spin-ladders also exist but iron has, in contrast to the former two examples, a heteroleptic tetrahedral coordination to three *Ch* and one O. Strong anti-ferromagnetic spin-spin interactions are reported for all four members of this compound series and iron is divalent and possesses a high-spin state (d^6, $S = 2$), as a consequence of the relatively small crystal field from the tetrahedral coordination. Recent investigations on $BaFe_2Se_2O$ reveal that its spin-ladder lattice transform to a layered lattice on performing the synthesis at high pressure.[7] Also, neutron diffraction data reveal an anti-ferromagnetic G-type order in that high-pressure modification.[7] However, to our knowledge, no one investigated the spin structure of ambient pressure modifications of $AEFe_2Ch_2O$ (*AE* = Ba, Sr; *Ch* = S, Se),[3-6] although anti-ferromagnetic spin-structure predictions were presented.[3] Hence, we performed Mössbauer spectroscopy and neutron diffraction experiments on powders of $SrFe_2Ch_2O$ (*Ch* = S, Se) and the results thereof will be presented here.

[a] Max Planck Institute for Chemical Physics of Solids
Nöthnitzer Straße 40, 01187 Dresden, Germany
Fax: +49-351-464644902
E-mail: martin.valldor@cpfs.mpg.de, m.valldor@ifw-dresden.de
Homepage: http://www.cpfs.mpg.de/
[b] Institut Laue-Langewin (ILL), 71 avenue des Martyrs, F-38042, Grenoble Cedex 9, France
[c] University of British Columbia, 2329 West Mall, Vancouver, BC V6T 1Z4, Canada
[d] Leibniz Institute for Solid State and Materials Research Helmholtzstraße 20, 01069, Dresden, Germany

Results and Discussion

All the syntheses and basic properties of the title compounds were reported in an earlier paper.[6] By comparing powder neutron diffraction at temperatures above and below the magnetic transition temperatures for $SrFe_2S_2O$ (T_N = 216 K) and $SrFe_2Se_2O$ (T_N = 228 K), as estimated from previously reported specific heat data,[6] several conclusions can be drawn: First, the fact that the "background intensity" is lower below T_N is due to a transfer of diffuse scattering into Bragg intensities, which fits the observed magnetic phase transition (Figure S1, Supporting Information). Second, all obvious magnetic scattering intensities superimpose with the core scattering, i.e. the magnetic scattering does not form any superstructure reflections, suggesting that the spin ordering vector is *k* = [000] (Figure 1). The powder neutron diffraction data obtained at 10 K can be well simulated with core scattering of $SrFe_2Ch_2O$ (*Ch* = S, Se) and a *Pm´m´n´* antiferromagnetic spin structure (Figure 2). All other magnetic structures allowed by magnetic symmetry analysis can be excluded.

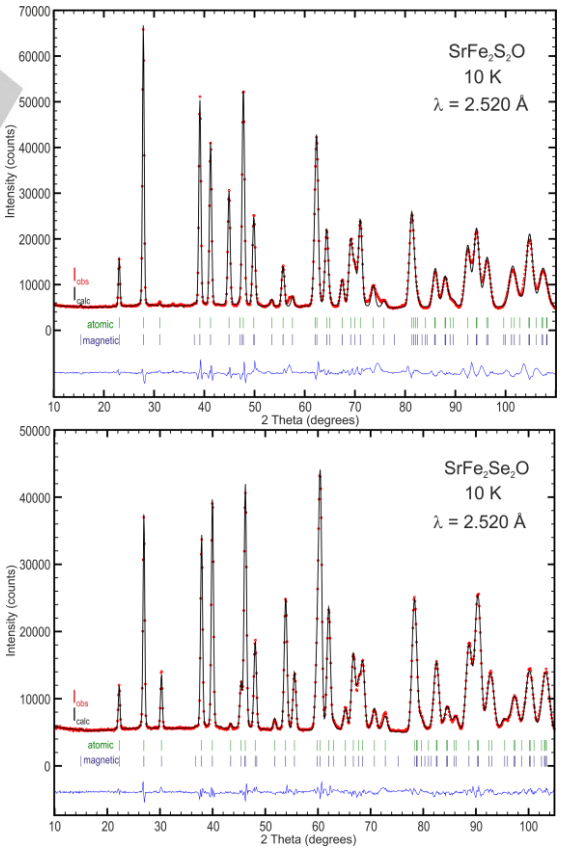

Figure 1. Rietveld refinement results of the crystal and magnetic structures of $SrFe_2S_2O$ (upper plot) and $SrFe_2Se_2O$ (lower plot).

The magnetic moments are aligned along the crystallographic *b*-axis with a small canted spin component along the crystallographic *c*-axis and the refined magnetic moments are close to 3.3 μ_B (*Ch* = S) and 3.5 μ_B (*Ch* = Se), which are below the expected spin-only ordered magnetic moment of 4 μ_B for high-spin Fe^{2+} (d^6) due to covalency. All further refined parameters can be found in Table 1.

Table 1. Refined parameters of the atomic and spin structure from powder neutron diffraction data of $SrFe_2Ch_2O$ (*Ch* = S, Se) at 10 K.

Compound	$SrFe_2S_2O$	$SrFe_2Se_2O$
Space group	*PmmnZ*	*PmmnZ*
Volume(Å^3)	228.9(1)	251.46(5)
T_N (K)	216	228
a (Å)	3.8695(7)	3.9908(5)
b (Å)	9.379(3)	9.648(1)
c (Å)	6.307(2)	6.5308(8)
Atom, *x*, *y*, *z*, *B*(iso)	Sr, ¼, ¼, 0.024(2),0.3(6) Fe, ¼, 0.582(1), 0.378(1), 0.3(3) S, ¼, 0.545(4), 0.743(4), 1(1) O, ¼, ¾, 0.218(3), 0.9(6)	Sr, ¼, ¼, 0.001(1),0.6(2) Fe, ¼, 0.5865(4), 0.3801(5), 1.11(7) Se, ¼, 0.5495(2), 0.7507(3), 1.1(2) O, ¼, ¾, 0.225(1), 1.3(3)
Fe–O–Fe	114.7(6)	114.6(4)
Fe–*Ch*–Fe (||)	107.7(5)	103.8(1)
Fe–*Ch*–Fe (⊥)	76.1(3)	75.1(1)
Fe–*Ch* (||)	2.40(3)	2.536(3)
Fe–*Ch* (⊥)	2.33(3)	2.446(4)
Fe–O	1.87(1)	1.875(6)
R_{Bragg}	0.0357	0.0842
R_F	0.0284	0.0657
Magnetic Symmetry	*Pm´m´n´*	*Pm´m´n´*
k-vector	[0,0,0]	[0,0,0]
Spin size (μ_B)	3.31	3.46
|Spin| along *a*, *b*, *c* (μ_B)	0, 3.3(1), 0.3(2)	0, 3.45(6), 0.2(1)
$R_{Magn.}$	0.0559	0.0491

Bond lengths (Å) and angles (°). All standard deviations are multiplied with the Berar-Lelann factor. || symbols the interaction along the ladder and ⊥ between ladders along the *c*-axis.

The observed spin structures in $SrFe_2Ch_2O$ (*Ch* = S, Se) can be described with ferromagnetic spin-spin interactions along the ladder lattice via *Ch*, which was suggested by Han et al.[3] for $BaFe_2Se_2O$. However, the same authors suggested three different anti-ferromagnetic ground states that do not agree with our data (Figure 2). Han et al. did predict anti-ferromagnetic coupling via O across the ladder rung in 2 out of 3 models (AFM-2 and AFM-3)[3] but both those spin-structures differ from our observations: the main spin component should point towards the ladder centre and not out of the ladder plane (Figure 2). Hence, the measured spin structures disagree with the calculated ones. One explanation could be that the observed spin structure was not tried in a calculation and could be lower in energy. Another reason for this discrepancy could be that the Ba-analogue indeed has a different spin ground state than the Sr-analogues presented here.

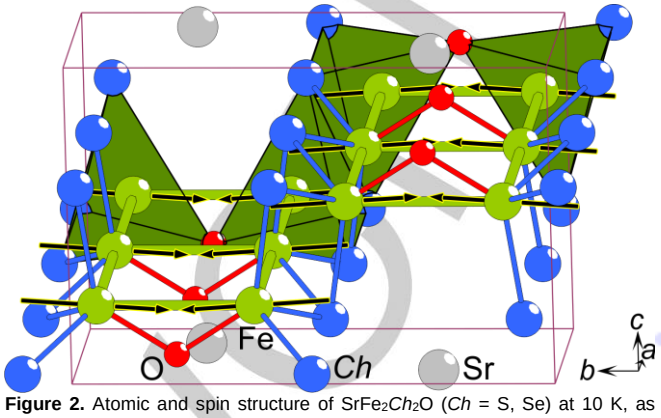

Figure 2. Atomic and spin structure of $SrFe_2Ch_2O$ (*Ch* = S, Se) at 10 K, as refined from neutron powder diffraction data. Unit cell is marked with thin lines and the tetrahedral Fe coordination is emphasized with polyhedra and bonds. The ladder lattice is marked with thinker lines that connect the Fe atoms.

As expected from thermal expansion, all cell parameters for both title compounds are significantly smaller at 10 K (Table 1) than at higher temperatures, as reported in Supporting information S1, S2, and elsewhere.[6] Note, at 10 K, the Fe–O–Fe bridge is, within experimental errors, identical for both title compounds: the Fe–O distances are 1.87(1) Å and the Fe–O–Fe angle is either 114.7(6)° (*Ch* = S) or 114.6(4)° (*Ch* = Se), see Table 1. These parameters suggest that the magnetic super-exchange across the rung should be similar in both compounds, which might be reflected in the same high temperature magnetic susceptibility – a broad maximum in $\chi(T)$ at about 550 K.[6] This can be concluded here because neutron diffraction data reveal the oxygen position with higher certainty compared to previous x-ray experiments. Hence, it might be more correct to assume local, singlet-like spin-dimer formation at high temperatures, above T_N, and the Néel ordering is mainly dependent on the strength of super-exchange interactions via Fe–*Ch*–Fe, along and between ladders. Here it is important to mention that the long-range anti-ferromagnetic order in the title compounds can only succeed, without any obvious breaking of crystallographic symmetries, if the spin-spin interaction along the ladders is ferromagnetic: with anti-ferromagnetic interactions along the ladders, a geometrical frustration would prevent the spin system to order, as in the case of $BaMn_2O_3$, where a breaking of crystallographic symmetry was necessary to allow for a magnetic ordering to set in.[8] From the crystallographic data (Table 1) it is possible to further examine the local coordination of Fe^{2+} (Figure 3). Due to its heteroleptic coordination and the size difference between O^{2-} and S^{2-}, Fe^{2+} is found 0.29 Å away from the geometric "charge barycenter" (CB). The result is a polar coordination for Fe^{2+}. Due to the possible single ion anisotropy of the high-spin d^6 electronic configuration, the polar coordination might have an influence on the direction of the ordered magnetic moments. Assuming the local polarity to be along the line between CB and the Fe-site, the angle between the magnetic spin orientation and coordination polarity is about 8° (see Figure 3).

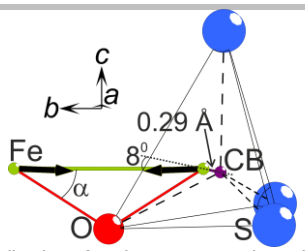

Figure 3. Local coordination of Fe in $SrFe_2S_2O$, where the ordered spins are marked, the charge barycenter (CB) is indicated, and the distance between CB and Fe-site is shown as well as the angle between the coordination polarity and the alignment of the magnetic moment (thick arrows).

The evolution of the magnetic order with temperature was followed for $SrFe_2S_2O$ by Mössbauer spectroscopy, where the *T*-dependence of the ordered magnetic moment of iron is reflected in the *T*-dependence of the magnetic hyperfine field B_{hf}. Some Mössbauer spectra of $SrFe_2S_2O$ and $SrFe_2Se_2O$, the data evaluation, and the interpretation of the Mössbauer parameters with respect to the electronic structure were already discussed previously.[6] Additional spectra of $SrFe_2S_2O$ are shown in Figure 4.

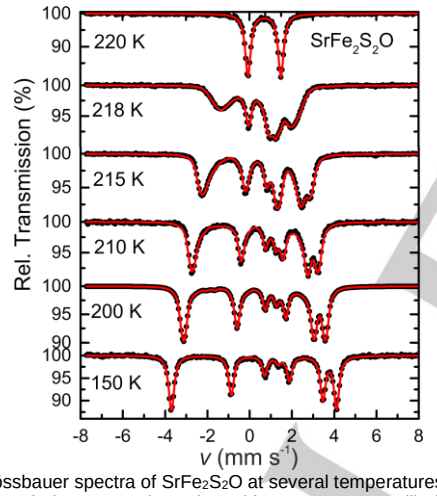

Figure 4. Mössbauer spectra of $SrFe_2S_2O$ at several temperatures highlighting the evolution of the magnetic order with temperature. Filled circles are measured data and solid lines (red) are calculated spectra obtained from the best fits.

The spectrum at 150 K was analysed using the full Hamiltonian including magnetic and quadrupolar hyperfine interactions and the transmission integral. Spectral shape and Mössbauer parameters are similar to those at 5 K[6] (Table 2), which indicates that crystal and magnetic structure remain unchanged. All spectra feature a single magnetic pattern, which is in agreement with the antiferromagnetic spin structure derived from the neutron data (Figure 2). The analysis of the 150 K spectrum confirms that the principal component V_{ZZ} of the electric field gradient (efg) is non-collinear with the direction of B_{hf}. The efg reflects the heteroleptic coordination environment of Fe^{2+} (Figure 3) and it is anticipated that the direction of V_{ZZ} is largely determined by the direction of the short Fe–O bond. The angle between Fe–Fe and Fe–O directions (α in Figure 3), the former essentially corresponding to the spin direction, is about 33°. This is not too far from the angle Ω between V_{ZZ} and B_{hf} of about 21°. In case of $SrFe_2Se_2O$, Ω ≈ 35° was obtained,[6] which is even closer to α.

Table 2. Mössbauer parameters obtained from the evaluation of the experimental spectra. Here, *IS*, *QS*, and B_{hf} correspond to the isomer shift, quadrupole splitting, and magnetic hyperfine field, respectively, η is the asymmetry parameter of the efg, and Ω the angle between the principal component V_{ZZ} of the efg and B_{hf}. The azimuthal angle is kept at zero.

T (K)	*IS* (mm s^{-1})	*QS* (mm s^{-1})	B_{hf} (T)	η	Ω (°)
220	0.711(1)	1.559(2)	-	-	-
218[a]	0.709(1)	–1.56(2)[b]	8.5	1[c]	22.0(3)
215[a]	0.709(1)	-1.67(2)[b]	13.9	1[c]	21.0(1)
210[a]	0.717(1)	-1.67(2)[b]	17.0	1[c]	21.5(1)
200[a]	0.728(1)	-1.66(2)[b]	19.7	1[c]	21.4(1)
150	0.753(1)	-1.69(2)[b]	23.2(1)	1[c]	21.1(1)

[a] Spectrum was evaluated with a distribution of hyperfine fields. B_{hf} here is the peak (most probable) hyperfine field. Note, for comparisons, in Ref.[6], the average B_{hf} value was given.
[b] In these spectra QS was calculated according to $QS = eQV_{ZZ}/2\ (1+\eta^2/3)^{1/2}$, where Q is the quadrupole moment of the excited ^{57}Fe nucleus.
[c] Limiting value. The asymmetry parameter was restricted to the range $0 \le \eta \le 1$.

When approaching the temperature region of the AFM – paramagnetic transition (200 K ≤ *T* < 220 K) the spectra become significantly broadened which was taken into account by a hyperfine field distribution (extracted by the Hesse-Rübartsch method[9]) within the thin absorber approximation. The reduced hyperfine fields $B_{hf}(T)/B_{hf}(0)$ are depicted in Figure 5 (left), where $B_{hf}(0) \approx B_{hf}(5\ K) = 25.1$ T[6] and in case of a B_{hf} distribution, the peak B_{hf} (most probable B_{hf}) values were used. It is apparent that B_{hf} decreases sharply between 200 and 220 K, in agreement with the Néel temperature of 218 K obtained from magnetisation data[6] and with the temperature dependent intensity of the partly magnetic (0 1 1) peak from the neutron diffraction data (Figure 5 right). In the critical region 200 K ≤ *T* < 220 K a power law fit $B_{hf}(T)/B_{hf}(0) = C\cdot(1 - T/T_N)^{\beta}$ was performed on the Mössbauer data Though in view of the limited number of data points this analysis should be taken with caution the resulting value for β is significantly smaller than β ≈ 1/3 expected for three-dimensional antiferromagnets. This is an indication for the low-dimensional nature of the magnetism in $SrFe_2S_2O$.

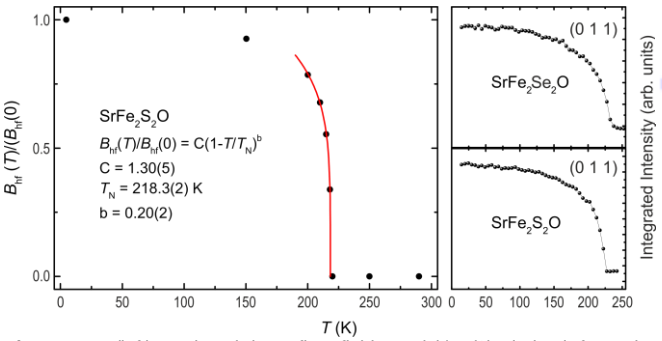

Figure 5. (left) Reduced hyperfine fields $B_{hf}(T)/B_{hf}(0)$ derived from the Mössbauer data of $SrFe_2S_2O$. Data in the critical region (200 K ≤ *T* < 220 K) were evaluated with the indicated power law. (right) Integrated neutron diffraction intensity at Bragg position (0 1 1) vs. temperature for both title compounds.

As iron containing spin ladder compounds are stated to be "promising material platforms" for novel superconductors,[2] it is important to compare new iron spin-ladders with the reported $BaFe_2S_3$ that superconducts under pressure: $BaFe_2S_3$ is chemically similar to $BaFe_2S_2O$[5] which is isostructural to the title compounds. However, the spin-ladders in $BaFe_2S_3$ form quasi-1D chains of homoleptically coordinated $[FeS_{2/2}S_{2/4}]^-$. In the title compounds, oxygen seems to make the crucial difference by causing a heteroleptic FeS_3O coordination, which also induces an electric polarity at the Fe-site. Moreover, oxygen increases the electronic correlations as a consequence of its higher electronegativity, as compared to sulfur; This lowers covalency and self-doping that are important parameters for the pressure induced superconductivity in $BaFe_2S_3$, as suggested by first principles calculation.[10] At normal pressures, $BaFe_2S_3$ exhibits a long range antiferromagnetic spin-order with the main moment along the Fe–Fe rung, but the spin-spin interaction across the rung is ferromagnetic and antiferromagnetic along the ladder.[2] This is completely reversed in $SrFe_2Ch_2O$ (*Ch* = S, Se), where the short Fe–O–Fe bridge drives strong antiferromagnetic interactions along the rungs. Hence, the spin ladders in the title compounds are clearly different from those in $BaFe_2S_3$. Iron containing spin-ladders seem to be very diverse indeed, and their detailed physical properties depend on local Fe-coordinations, the electronic correlation strengths, as well as the crystal structures.

Conclusions

Long range anti-ferromagnetic spin orderings with k = [0,0,0] are found in $SrFe_2Ch_2O$ (*Ch* = S, Se), as probed by powder neutron diffraction and Mössbauer spectroscopy. Within the spin-ladder lattice, the super-exchange interaction across each rung via oxygen is antiferromagnetic but ferromagnetic along the ladders via *Ch*; the interaction signs are reversed as compared to the spin-ladder compound $BaFe_2S_3$. In both title compounds, the ordered spins point towards the center of the ladders, which is different than predicted from density functional theory calculations.

Experimental Section

Powder neutron diffraction measurements have been performed at the D1B diffractometer at the ILL in Grenoble, France (λ = 2.52 Å). The Fullprof program suite[11] was used for Rietveld refinement.

Mössbauer spectra of $SrFe_2S_2O$ and $SrFe_2Se_2O$ were collected and evaluated as described previously,[6] including the use of the Winmoss software.[12]

Acknowledgements

This work was supported by the German Science Foundation (DFG) through SFB1143.

Keywords: Iron • Neutron scattering • Magnetic structure • Mössbauer spectroscopy

[1] F. -C. Hsu, J. -Y. Luo, K. -W. Yeh, T. -K. Chen, T. -W. Huang, P. M. Wu, Y. -C. Lee, Y. -L. Huang, Y. -Y. Chu, D. -C. Yan, M. -K. Wu, *Proc. Natl. Acad. Sci. USA* **2008**, *105*, 14262–14264.

[2] H. Takahashi, A. Sugimoto, Y. Nambu, T. Yamauchi, Y. Hirata, T. Kawakami, M. Avdeev, K. Matsubayashi, F. Du, C. Kawashima, H. Soeda, S. Nakano, Y. Uwatoko, Y. Ueda, T. J. Sato, K. Ohgushi, *Nat. Mater.* **2015**, *14*, 1008–1013.

[3] F. Han, X. Wan, B. Shen, H. Wen, *Phys. Rev. B* **2012**, *86*, 014411.

[4] H. Lei, H. Ryu, V. Ivanovski, J. B. Warren, A. I. Frenkel, B. Cekic, W. Yin, C. Petrovic, *Phys. Rev. B* **2012**, *86*, 195133.

[5] M. Valldor, P. Adler, Yu. Prots, U. Burkhardt, L. H. Tjeng, *Eur. J. Inorg. Chem.* **2014**, *36*, 6150–6155.

[6] S. Huh, Yu. Prots, P. Adler, L. H. Tjeng, M. Valldor, M. *Eur. J. Inorg. Chem.* **2015**, *2015*, 2982.

[7] F. Takeiri, Y. Matsumoto, T. Yamamoto, N. Hayashi, Z. Li, T. Tohyama, C. Tassel, C. Ritter, Y. Narumi, M. Hagiwara, H. Kageyama, *Phys. Rev. B* **2016**, *94*, 184426.

[8] M. Valldor, O. Heyer, A. C. Komarek, M. Braden, T. Lorenz, *Phys. Rev. B* **2011**, *83*, 024418.

[9] J. Hesse, A. Rübartsch, *J. Phys. E: Sci. Instrum.* **1974**, *7*, 526–532.

[10] Y. Zhang, L. Lin, J.-J. Zhang, E. Dagotto, S. Dong, *Phys. Rev. B* **2017**, *95*, 115154.

[11] J. Rodríguez-Carvajal, *Phys. B* **1993**, *192*, 55–69.

[12] Z. Klencsár, A. Kuzmann, A. Vértes, *J. Radioanal. Nucl. Chem.* **1996**, *210(1)*, 105–118.

WILEY-VCH

Entry for the Table of Contents

FULL PAPER

$SrFe_2Ch_2O$ (*Ch* = S, Se) exhibit long-range antiferromagnetic ordering on spin ladders. Across the rung, an oxygen ion bridges for anti-ferromagnetic spin interactions while ferromagnetic interactions dominate along and between ladders via *Ch*. Mössbauer data suggest that the local electric field gradient at the Fe-site is dominated by the Fe–O bond in the $FeCh_3O$ tetrahedron.

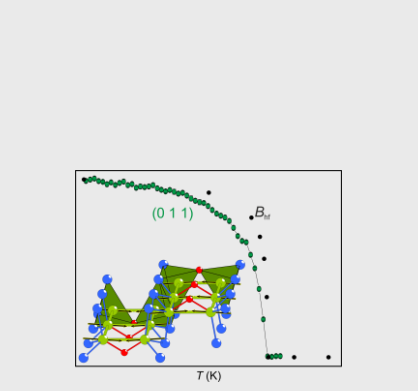

*Hanjie Guo, Maria-Teresa Fernández-Díaz, Alexander Christoph Komarek, Sungjoon Huh, Peter Adler, Martin Valldor**

Page No. – Page No.

Long-range anti-ferromagnetic order on spin ladders $SrFe_2S_2O$ and $SrFe_2Se_2O$, as probed by neutron diffraction and Mössbauer spectroscopy